Laser and Particle Beams (2017), *35*, 313–325.

doi:10.1017/S0263034617000210

Spatial confinement effects employed by metallic blocker and Ar gas pressures on laser-induced breakdown spectroscopy and surface modifications of laser-irradiated Mg

A. HAYAT,[1] S. BASHIR,[1] M. S. RAFIQUE,[2] R. AHMED,[1] M. AKRAM,[1] K. MAHMOOD,[1] A. ZAHEER,[1] T. HUSSAIN,[1] AND A. DAWOOD[1]

[1]Centre for Advanced Studies in Physics, GC University, Lahore, Pakistan
[2]Department of Physics, University of Engineering and Technology, Lahore, Pakistan

(RECEIVED 1 February 2017; ACCEPTED 20 February 2017)

Abstract

Spatial confinement effects on plasma parameters and surface morphology of laser-ablated Mg are studied by introducing a metallic blocker as well as argon (Ar) gas at different pressures. Nd: YAG laser at various fluences ranging from 7 to 28 J/cm^2 was employed to generate Mg plasma. Confinement effects offered by metallic blocker are investigated by placing the blocker at different distances of 6, 8, and 10 mm from the target surface; whereas spatial confinement offered by environmental gas is explored under four different pressures of 5, 10, 20, and 50 Torr. Laser-induced breakdown spectroscopy analysis revealed that both plasma parameters, that is, excitation temperature and electron number density initially are strongly dependent upon both pressures of environmental gases and distances of blockers. The maximum electron temperature of Mg plasma is achieved at Ar gas pressure of 20 Torr, whereas maximum electron number density is achieved at 50 Torr. It is also observed that spatial confinement offered by metallic blocker is responsible for the significant enhancement of both electron temperature and electron number density of Mg plasma. Maximum values of electron temperature and electron number density without blocker are 8335 K and 2.4×10^{16} cm^{-3}, respectively, whereas these values are enhanced to 12,200 K and 4×10^{16} cm^{-3} in the presence of blocker. Physical mechanisms responsible for the enhancement of Mg plasma parameters are plasma compression, confinement and pronounced collisional excitations due to reflection of shock waves. Scanning electron microscope analysis was performed to explore the surface morphology of laser-ablated Mg. It reveals the formation of ripples and channels that become more distinct in the presence of blocker due to plasma confinement. The optimum combination of blocker distance, fluence and Ar pressure can identify the suitable conditions for defining the role of plasma parameters for surface structuring.

Keywords: Electron number density; Electron temperature; Laser-induced breakdown spectroscopy; Spatial confinement; Spectral emissions

1. INTRODUCTION

Laser-induced breakdown spectroscopy (LIBS) is a rapidly developing and emerging technique for spectrochemical analysis of materials and plasma diagnostics (Cremer & Radziemski, 2006; Khumaeni *et al.*, 2016). Multi-elemental analysis of almost all kinds of samples including solids, liquids and gases with minimum sample preparation, capability of micro-area analysis, and real-time detection are promising aspects of this popular technique. Therefore, LIBS is widely applicable in different areas of research, manufacturing industry, medicine, and space sciences (Zhong *et al.*, 2016). In this technique, a highly focused pulsed laser beam is employed as an excitation source to generate a high-temperature and high-density plasma (Scaffidi *et al.*, 2003; Khumaeni *et al.*, 2016). The elemental composition as well as the electron temperature and electron number density of laser-assisted plasma is evaluated by the analysis of the selective atomic and molecular emissions from excited plasma (Harilal *et al.*, 2014). However, as compared with other spectroscopic methods, LIBS always suffers from relatively poor detection

Address correspondence and reprint requests to: A. Hayat, Centre for Advanced Studies in Physics, GC University, Lahore, Pakistan. E-mail: asmahayat@gcu.edu.pk

sensitivity. Different techniques have been adopted by various research groups to enhance the detection efficiency and to improve the surface structuring, for example, by optimizing the laser parameters and by enhancing the plasma confinement effects (Liu *et al.*, 2015). The increased ablation rate, longer plasma duration, and higher plasma temperature are responsible for the enhancement of line emission intensity, improved detection capability, and surface structuring of irradiated targets.

Among these methods, the most common approach for the enhancement of LIBS sensitivity and ablation efficiency is control over nature and pressure of environmental gases. It introduces the spatial confinement effects on plasma plume expansion. The presence of environmental gases restricts the free expansion of plasma species resulting in significant confinement effects on plasma parameters. Farid *et al.* (2014) studied the effect of ambient gas pressure from vacuum to 760 Torr on copper plasma parameters and attained the maximum electron temperature at 300 Torr due to maximum decrease in plume length. Our group (Dawood *et al.*, 2015) also investigated the effect of nature and pressures of ambient gases (He, Ne, Ar) on electron temperature and electron number density of laser-induced Mg alloy plasma. The highest values of emission intensity, electron temperature, electron number density, and material microhardness were observed in the presence of Ar environment as compared with He and Ne. More recently, Shakeel *et al.* (2016) investigated the effect of ambient pressures and laser irradiance of Nd: YAG laser at 1064 nm on germanium plasma parameters and found the improved analytical performance of LIBS through the variation of ambient pressure from 8 to 250 mbar and laser irradiance from 9 to 33 GW cm^{-2}.

Spatial confinement is another suitable suggested technique for increasing the detection efficiency of LIBS and ablation mechanisms. It plays an effective role for increasing plasma shock wave pressure (Harilal *et al.*, 2014). There are various experimental techniques which can be employed for the compression and confinement of plasma, for example, environmental gas and their pressures (Dawood & Margot, 2014), presence of electric and magnetic field (Fried *et al.*, 1992), plasma plume collisions with obstructing surfaces (Gao *et al.*, 2015), double pulse discharge enhancement (Chen *et al.*, 2015), drilling and irregular configurations of target surface, etc. (Fu *et al.*, 2016). All these methods have shown a strong influence upon incident laser-target coupling, expanding plume dynamics and plume interaction with target surface (Khalil & Gondal, 2012; Harilal *et al.*, 2014).

The spatial confinement offered by obstructing surface in LIBS technique has attained a lot of attention from researchers (Huang *et al.*, 2015). It has found to be effective for the significant enhancement of emission intensity, electron temperature, and number density. In the presence of a small obstructing surface placed across the plume expansion path, a propagated shock wave during plasma expansion is reflected back from this immobile obstructing surface and is responsible to modify the plasma shape, size, lifetime, and dynamics (Fu *et al.*, 2016). This arrangement results in additional process such as enhanced emissions and enhanced recombination rates at collisional surface that finally leads to a large gradient in electron temperature and electron number density. For such type of plasma confinement, a number of scientific groups have adopted different configurations of obstructing surface (Huang *et al.*, 2015). Gao *et al.* (2015) used pair of parallel aluminum (Al) plates as confining surfaces for Cu plasma and found 10 mm best distance for enhancement of electron temperature and electron number density. More recently, Fu *et al.* (2016) explored physical effects of cavity on enhancement of LIBS spectra of Brass target on the basis of reflected shock wave compression effects.

The aim of present work is to investigate the spatial confinement effects on Mg plasma parameters (electron temperature and electron number density) and surface morphology. The variation in electron temperature and number density has been evaluated by LIBS analysis, whereas surface modification of irradiated Mg has been analyzed using scanning electron microscope (SEM).

To the best of our knowledge, no comparative study of LIBS and surface modification of Mg at various fluences, Ar pressures and blocker distances has yet been reported. Two techniques are employed for the spatial confinement of Mg plasma. One is by introducing Ar gas at different pressures ranging from 5 to 50 Torr. The second technique employed for the spatial confinement of Mg plasma is introducing an Al-metallic blocker which is placed at three different distances of 6, 8, and 10 mm from the target surface. The electron temperature and electron number density are evaluated for all pressures in the absence and presence of blocker at different distances of 6, 8, and 10 mm at laser fluence ranging from 7 to 28 J/cm^2. The aim is to investigate the most suitable and optimum combination of laser fluence, Ar gas pressure and Al blocker distance for the enhancement of kinetic energy and charge density of ablated species of Mg which in turn are responsible for the surface modification of Mg. The optimum control over plasma parameters with pronounced spatial confinement effects makes plasma more suitable for thin-film deposition, ion implantation as well as micro/nano-structuring of materials.

2. EXPERIMENTAL DETAILS

The schematic of experimental setup used for laser-assisted ablation and plasma generation of Mg is illustrated in Figure 1. Circular-shaped disc of Mg (99.99, Alpha Aesar) with diameter of 33 mm, and thickness of 8 mm were selected as target material. The mechanically polished and ultrasonically cleaned Mg targets were placed at a distance of 3 mm before the focus in order to minimize the breakdown of ambient gas. The laser beam was focused on to the Mg surface at normal incidence by a 50 cm focal length lens. The estimated area of the laser spot on target was 7×10^{-3} cm^2, which was measured by SEM analysis. Samples were mounted on a motorized rotating stage for the analysis of fresh sample surface for each exposure in order to improve the

https://doi.org/10.1017/S0263034617000210 Published online by Cambridge University Press

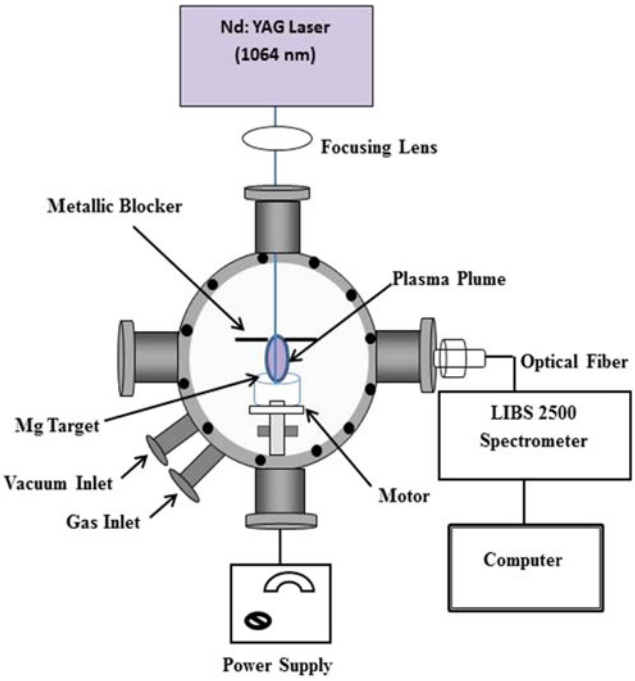

Fig. 1. The schematic of experimental setup for laser-induced breakdown spectroscopy of Mg plasma. Al plate was used as a reflector (blocker) of shock waves for spatial confinement of plasma.

reproducibility and accuracy of the spectral emission lines. A Q-switched Nd: YAG laser (CFR 200 Big Sky Laser Technologies Quantel France) with wavelength of 1064 nm, pulse duration of 10 ns, pulse energy of 25–200 mJ, with repetition rate of 1–10 Hz was employed for ablation and plasma formation. The emissions from Mg plasma were collected by LIBS 2500 plus spectrometer system (Ocean Optics Inc, USA) consisting of LIBS fiber bundle with seven linear silicon CCD (charge-coupled device) array detectors for a broad band 200–980 nm analysis. The optical resolution of LIBS system was 0.1 nm. All the measurements were performed with a time window (integration time) of the order of 2.1 ms and delay time 2.01 μs.

In order to introduce spatial confinement effects to Mg plasma, an experimental setup was designed and fabricated. It consists of a square Al plate of dimensions $5 \times 8 \times 0.1$ cm^3 that was inserted as a blocker between the target and the laser beam. The blocker was placed on the holder which was attached to a micro-positioner to control the distance of the plate from target surface. A small hole of diameter 4 mm was drilled in the center of Al plate to allow laser beam to pass and to interact normally with the target surface to produce plasma. For appropriate alignment with laser and target surface, both the target holder and blocker holder were placed on the same base.

In order to investigate the effect of laser fluence and spatial confinement on LIBS and surface morphology of ablated Mg, following three sets of experiments were performed.

(1) The first set of experiment was performed for LIBS analysis of Mg plasma. For this purpose, the targets were exposed to a single laser shot of Nd: YAG laser at four various Ar pressures of 5, 10, 20, and 50 Torr, which were accurately measured by a pressure gauge of mbar precision. The laser fluence was varied by varying the laser energy from 50 to 200 mJ for each pressure value by simply changing the delay time between flash lamps and Q-switch that corresponds to laser fluence ranging from 7 to 28 J/cm^2, respectively. Mg plasma was generated in a vacuum chamber.

(2) In the second set of experiment, samples were exposed under the same experimental conditions as have been employed for the first set of experiment except additional introduction of metallic blocker that was placed at three various distances of 6, 8, and 10 mm. We also performed the same set of experiment for blocker distance of 2 and 4 mm but no emission enhancement was found to be observed. The experiments were also performed for Ar pressure of value greater than 50 Torr. No significant enhancement in emission signals was observed even at higher energies with different blocker distances for the pressure >50 Torr. Therefore the data presented in results and discussion part deals with the Mg plasma generated in Ar gas at pressure of 5, 10, 20, and 50 Torr. The results at higher pressures are not presented. Similarly, the results related to blocker distance of <6 mm are also not reported in the present paper.

(3) In order to correlate the electron temperature and electron number density explored by LIBS analysis with surface modifications, SEM analysis of laser-irradiated Mg was performed. The surface morphology of irradiated Mg samples was explored by using SEM (JEOL JSM-6480 LV).

For the SEM analysis, freshly polished and ultrasonically cleaned targets were exposed to laser pulses of Nd: YAG laser at only one fluence. The choice of this fluence value is based on the evaluation of electron temperature of Mg plasma by Boltzmann plot method (Section 3.1.1). This higher value of fluence is chosen where the maximum value of electron temperature is obtained for Mg plasma.

3. RESULTS AND DISCUSSION

3.1. LIBS analysis for Mg plasma parameters

The emission spectra of Mg illustrated in Figure 2 reveals the effects on emission intensity in the absence (Fig. 2a, 2b) and in the presence of metallic blocker at a distance of 6 mm (Fig. 2c) and at a distance of 8 mm (Fig. 2d) obtained under Ar pressure of 20 Torr at a laser fluence of 18 J/cm^2. The comparison of Figure 2a–2d clearly indicates that plasma intensities are significantly enhanced in the presence of metal blocker that is used as a confining and reflecting surface for expanding shock waves and plasma plume. In order to study the

https://doi.org/10.1017/S0263034617000210 Published online by Cambridge University Press

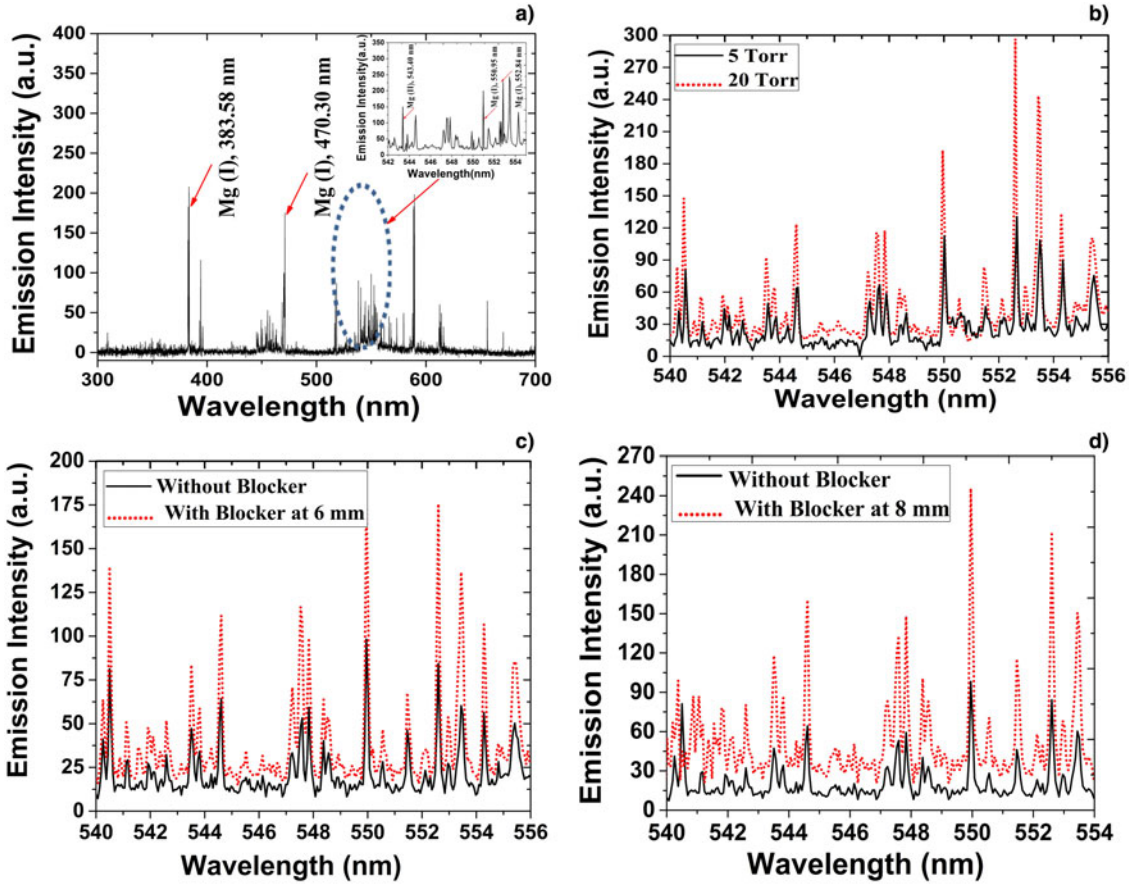

Fig. 2. The emission spectra of laser- induced Mg plasma (a-b) without blocker and with Al blocker at a distance of (c) 6 mm and (d) 8 mm under Ar gas pressure of 20 Torr at a laser fluence of 18 J/cm^2 identified by LIBS spectrometer system.

effects of laser fluence and blocker distance on excitation temperature and electron number density of Mg plasma, with and without blocker, the five spectral lines of Mg (I) 383.53, Mg (I) 470.30, Mg (II) 543.40, Mg (I) 550.95, and Mg (I) 552.84 nm were selected and are labeled in Figure 2a and in its inset (Chorlis *et al.*, 1980). LIBS spectra of laser-ablated Mg plasma were obtained with the help of LIBS2500 spectrometer having spectral range from 200 to 900 nm. The laser fluence was varied from 7 to 28 J/cm^2 at four different Ar pressures of 5, 10, 20, and 50 Torr. All the measurements were taken in the absence and presence of metallic blocker.

3.1.1. Electron temperature

The electron temperature and electron number density are two important plasma parameters which are essential for consideration of dissociation, excitation and ionization processes of plasma. The obtained emission spectra are used to calculate electron temperature and density of laser-induced Mg plasma. Electron temperature is calculated with the help of well-known Boltzmann plot method (Hayat *et al.*, 2016),

$$\ln\left(\frac{\lambda_{mn} I_{mn}}{g_m A_{mn}}\right) = -\frac{E_m}{kT_e} + \ln\left(\frac{N(T)}{U(T)}\right), \quad (1)$$

where I_{mn}, λ_{mn}, A_{mn}, g_m, and E_m are the intensity, wavelength, transition probability, statistical weight, and energy of upper state m, respectively. $U(T)$, $N(T)$, k, and T_e are the partition function, total number density, Boltzmann constant, and electron temperature, respectively. For a given spectrum, a Boltzmann plot of the logarithmic term ($\lambda_{mn} I_{mn}/g_m A_{mn}$) versus E_m yields a straight line whose slope is equal to $-1/kT_e$. The intensities of five various selected Mg lines are used for Boltzmann distribution. The relevant spectroscopic data for these is listed in Table 1 (Chorlis *et al.*, 1980).

Table 1. *Relevant spectroscopic data of laser-ablated Mg plasma taken from literature (Chorlis* et al.*, 1980).*

Wavelength (nm)	Transitions	Energy of upper level, E_m (cm^{-1})	Statistical weight (g)	Transition probabilities (108 S^{-1})
383.53	3*s*3*p*−3*s*3*d*	47957	15	1.68
470.30	3*s*3*p*−3*s*5*d*	56308	5	0.255
543.40	2*p*7*d*–2*p*4*f*	112197	4	0.00245
550.95	3*s*8*p*–3*s*4*s*	59342	5	1.785 e5
552.84	3*s*4*d*–3*s*3*p*	53134	5	0.104

https://doi.org/10.1017/S0263034617000210 Published online by Cambridge University Press

3.1.2. Electron number density

For the evaluation of electron density of Mg plasma, most widely utilized spectroscopic technique is stark width broadening. However, by considering local thermal equilibrium (LTE) condition, a Lorentzian function was used to evaluate the full width at half maximum (FWHM) of stark-broadened lines for the plasma number density calculations (Zhong *et al.*, 2016). Doppler broadening mechanism is completely negligible in comparison with broadening caused by the charged particle (Stark broadening). This line broadening is more important for the determination of electron density. The electron density related to the FWHM of stark broadened line $\Delta\lambda_{1/2}$ nm, is given by the following relation (Harilal *et al.*, 2016),

$$\Delta\lambda_{1/2} = 2\omega\left(\frac{N_e}{10^{16}}\right) + 3.5A\left(\frac{N_e}{10^{16}}\right)^{1/4}\left[1 - 1.2N_D^{-1/3}\right] \times \omega\left(\frac{N_e}{10^{16}}\right), \quad (2)$$

where N_e is the electron number density (cm^{-3}), ω is the electron impact width parameter, and A is the ion-broadening parameter. Both ω and A are weak functions of temperature and can be interpolated at different temperatures by using quadratic relation. The first term in Eq. (2) refers to the electron broadening and second term is the contribution from the ion broadening, which is very small (in our case) and can be neglected and Eq. (2) reduces to (Chen *et al.*, 2015),

$$N_e = \left(\frac{\Delta\lambda_{1/2}}{2\omega}\right) \times 10^{16}\ cm^{-3}. \quad (3)$$

Using Eq. (3), electron density is calculated by Stark broadening of Mg I at 470.30 nm, which is well isolated, and fulfills the criteria of minimum self-absorption. For the validity of this method, plasma is assumed to be consisting of single-electron temperature under LTE condition. It is well known that McWhirter criteria is a necessary but insufficient condition often used for the verification of existence of LTE condition and exists if (Shakeel *et al.*, 2016),

$$N_e \geq 1.6 \times 10^{12} T_e^{1/2} \Delta E^3\ cm^{-3}. \quad (4)$$

According to which the minimum electron number density has been estimated to be 10^{12} cm^{-3}. Our minimum calculated values of electron number density for all measurements are 10^{16} cm^{-3} that are much greater than that required by McWhirter criterion for LTE.

3.1.3. Effect of ambient nature and its pressure on the plasma parameters

The effect of Ar gas pressure on Mg plasma parameters at seven different laser fluences ranging from 7 to 28 J/cm^2 is revealed in graphs of Figure 3 (without blocker), Figure 4 (at blocker distance of 6 mm), Figure 5 (at blocker distance of 8 mm) and Figure 6 (at blocker distance of 8 mm). The graphs of Figures 3a, 4a, 5a, and 6a represent the variation in electron temperature of Mg plasma with Ar gas pressure, whereas Figures 3b, 4b, 5b, and 6b represent the variation in electron number density of Mg plasma. It is clear from these figures that both electron temperature and electron number density are characterized by initial rise with increasing Ar pressure for all fluence values. The maximum value of electron temperature is achieved at a pressure of 20 Torr and it decreases at maximum pressure of 50 Torr for all measurements. On the other hand, electron number density increases with increasing Ar gas pressure up to a maximum value of 50 Torr. The statistical errors for determination of excitation temperature and electron number density are <5%. This increase in both plasma parameters, that is, electron temperature and electron number density with increasing background pressure is attributed to enhanced ablation rate and confinement effects (Harilal *et al.*, 2014). The decrease in electron temperature at maximum value of Ar pressure is

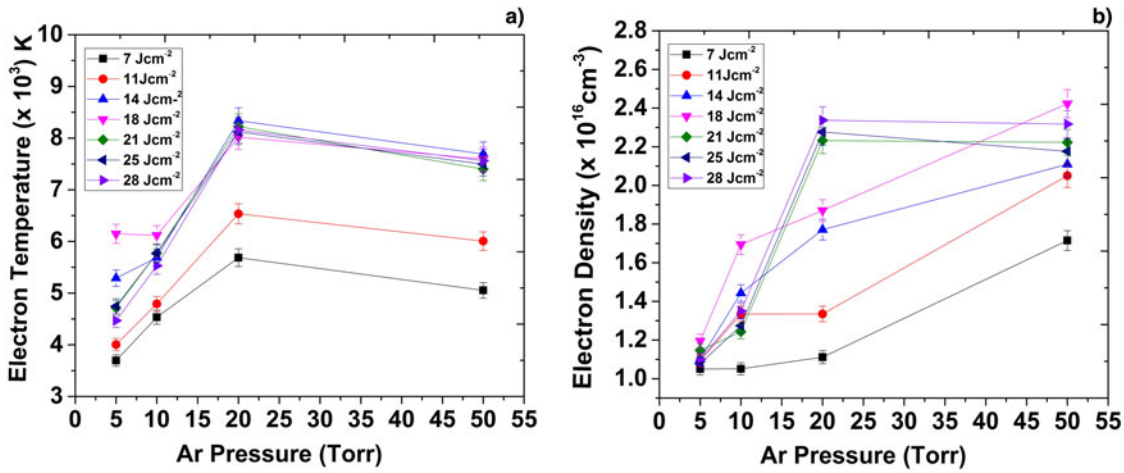

Fig. 3. The variation in (a) excitation temperature and (b) electron number density of laser-induced Mg plasma without blocker at various Ar gas pressures ranging from 5–50 Torr at laser fluences ranging from 7 to 28 J/cm^2.

https://doi.org/10.1017/S0263034617000210 Published online by Cambridge University Press

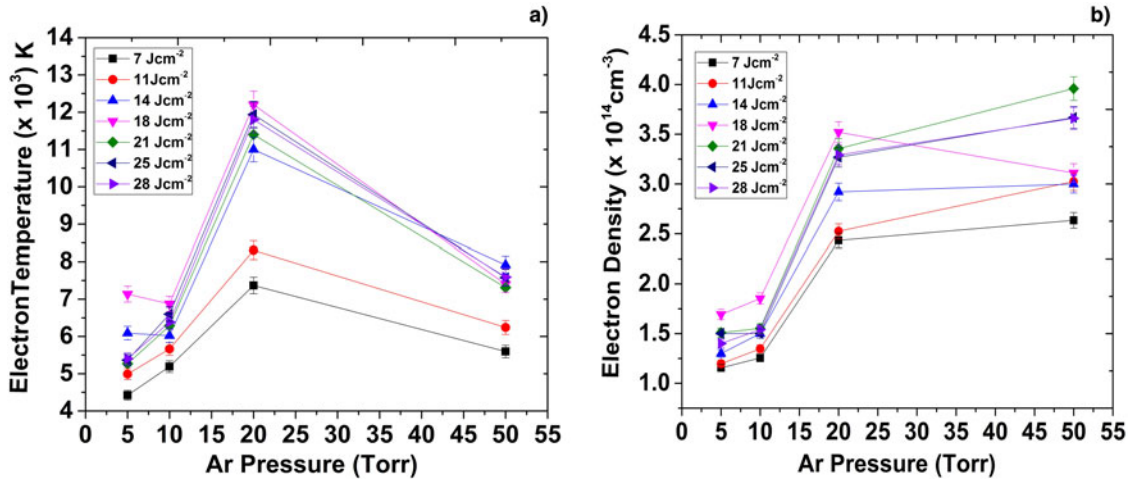

Fig. 4. The variation in (a) excitation temperature and (b) electron number density of laser-induced Mg plasma with blocker at distance of 6 mm at various Ar gas pressures ranging from 5–50 Torr at laser fluences ranging from 7 to 28 J/cm^2.

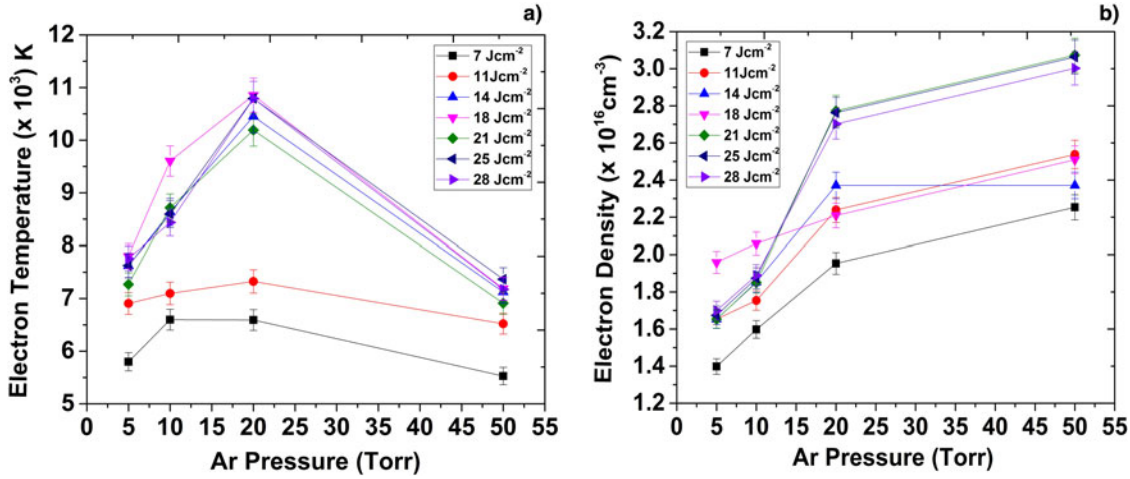

Fig. 5. The variation in (a) excitation temperature and (b) electron number density of laser-induced Mg plasma with blocker at distance of 8 mm at various Ar gas pressures ranging from 5–50 Torr at laser fluences ranging from 7 to 28 J/cm^2.

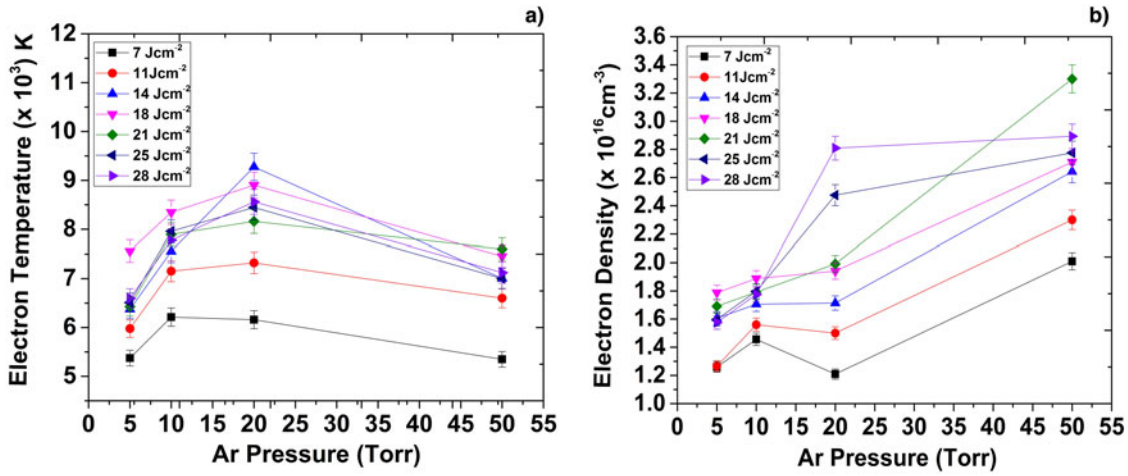

Fig. 6. The variation in (a) excitation temperature and (b) electron number density of laser-induced Mg plasma with blocker at distance of 10 mm at various Ar gas pressures ranging from 5–50 Torr at laser fluences ranging from 7 to 28 J/cm^2

https://doi.org/10.1017/S0263034617000210 Published online by Cambridge University Press

attributed to shielding effect and energy losses through collisional process.

It is a well-known fact that expansion of laser-induced plasma in the presence of ambient gas is strongly dependent upon plume energy, atomic mass, and number density of ambient gas. The presence of an ambient gas enhances the emissions from all plasma species depending upon its nature and pressure as well as on excitation energy of electronic transitions (Harilal *et al.*, 1998). The lifetime of all these transitions which lies of the order of a few nanosecond, is enhanced to few tens of nanosecond in the presence of ambient gas. This increase in transition lifetime is due to enhanced collisional processes (Verhoff *et al.*, 2012). Initially when nanosecond laser interacts with material, the maximum amount of laser energy is absorbed by the target. The plasma species generated by leading edge of beam near the target surface expand with high velocity of $\approx 10^4$–10^5 m/s for nanosecond laser and absorb the incoming energy through inverse bremsstrahlung (IB) and multiphoton ionization. The laser–plasma interactions (shielding effect) at trailing edge of laser pulse enhances the cascade-growth of plasma due to more energy absorption by free electrons through IB, which in turn increases the electron temperature and electron number density of nascent plasma.

These plasma parameters are strongly dependent upon IB coefficient $\propto_{\mathrm{IB}}$ given as (Farid *et al.*, 2014),

$$\propto_{\mathrm{IB}} = 1.37 \times 10^{-34} 3 n_e^2 \, T_e^{-1/2}, \tag{5}$$

where λ (nm) is the wavelength of incident laser, n_e (cm^{-3}) and T_e (K) are the electron density and electron temperature, respectively. At higher ambient pressure, the shielding and confinement of plasma through background gas become more dominant which results in hotter plasma generation due to more energy absorption by plasma through IB. At this stage, the plasma becomes more confined near to the target surface resulting in increase in frequency of effective electron collisions with more momentum transfer. Therefore the maximum value of electron temperature is obtained at pressure 20 Torr. The maximum value of electron number density obtained at pressure of 50 Torr is attributed to IB process, which has strong dependence upon plasma density (n_e^2) as compared with temperature $(T_e)^{-1/2}$ from Eq. (5). At this higher pressure of 50 Torr, the IB process becomes more favorable for enhancement of plasma density due to more laser energy coupling into the plasma, whereas decrease in electron temperature is related to the shielding effect which in turn reduce the laser absorption through target itself at higher value of Ar pressure. At higher Ar pressure of 50 Torr, strong shielding effect reduces the mass ablation rate and loss of electron energy into background atmosphere becomes dominant through elastic collisions given by following relation (Rumsby & Paul,1974),

$$Q_{\Delta t} = \frac{2m_e}{M_B} 6_{ea} n_B \sqrt{\frac{5KT_e}{\pi m_e}}, \tag{6}$$

where "m_e" and "M_B" are the masses of electron and background gas atoms, respectively. "6_{ea}" is scattering cross-section of elastic collision of electrons, and "n_B" is the density of background gas atoms. It is clear that cooling is dependent upon density of ambient gas. Therefore, at high pressure of 50 Torr of Ar, heat generated by confinement and laser-induced Mg plasma coupling is lost by higher collisional rate among plasma species and distribution of same amount of energy among larger number of particles finally reduces the localized plasma plume temperature.

3.1.4. Effect of metal blocker and its distance on plasma parameters

The target ablation and plasma formation in the presence of an immovable obstacle (metal blocker) can results in significant additional processes such as plasma shock wave pressure, enhanced emission at collisional surface and hydrodynamic interaction of expanding plasma plume with target. The obstacle surfaces are usually located at some distance from the target and are oriented parallel to it. The physical nature of spatial confinement effect through these surfaces is based on the theme that reflected shock waves from metal blocker compress the expanding plasma while increasing the collisional rate of particles.

The most direct way to evaluate the enhancement effect of electron temperature and electron number density is to compare these values in both presence and absence of blocker. For this purpose, spatial confinement effects on emission spectra of laser-induced Mg plasma are examined by placing the blocker at three different distances of 6, 8, and 10 mm from the target. Figures 3–6 represent the comparison of electron temperature and electron number density trends observed at different fluences under four various Ar pressures of 5, 10, 20, and 50 Torr without and with blocker at a distance of 6, 8, and 10 mm. It is observed that the Mg plasma temperature shows increasing trend with increasing pressure, attain their maxima at pressure 20 Torr and finally decreases at maximum pressure of 50 Torr for all measurements; whereas electron number density continuous to increase till the maximum pressure of 50 Torr for all measurements. These trends remain same for both cases either in the presence or absence of blocker. However, it is clearly seen that both plasma parameters are significantly enhanced in the presence of metallic blocker as compared with its absence. The values of these plasma parameters are also strongly dependent upon blocker distances.

The maximum value of electron temperature without block is 8335 K under Ar gas pressure of 20 Torr. This value shows the significant enhancement in the presence of blocker at all distances of 6, 8, and 10 mm and comes out to be 12,200, 10,854, and 9276 K, respectively. Similarly, the maximum value of electron number density without block is 2.4×10^{16} cm^{-3} under Ar pressure of 20 Torr. The value of electron number density is enhanced to 4×10^{16}, 3.1×10^{16} and 3.3×10^{16} cm^{-3} for blocker distance of 6, 8, and 10 mm, respectively. The higher electron temperature and electron

https://doi.org/10.1017/S0263034617000210 Published online by Cambridge University Press

number density values in presence of metallic block are explained on the basis of shock waves reflection from that metallic surface which after reflection, physically modifies the plasma plume into smaller space while providing additional energy to the vapor plume as compared with freely expanding plasma. This confinement leads to more condensed plasma core area with enhanced collisional rate, excitation/de-excitation and plasma emissions. It is reported (Gao *et al.*, 2015) that the plasma core position develops into the more spatially stable form after reflection from metallic surface placed at moderate distance. This causes the core part to become more homogeneous and results into high-temperature and high-density plasma. The presence of blocker also produces a significant effect on shock-affected area around ablated spot. The shock-affected region has clearly been observed in SEM micrographs and has been calculated ("SEM analysis" in Section 3.2).

In order to explain the results regarding the effect of blocker distance on Mg plasma parameters, the analysis is divided into two regimes. One regime deals with the lower pressures of Ar, that is, 5 and 10 Torr; whereas the second regime corresponds to higher Ar pressures, that is, 20 and 50 Torr. While comparing the distances of the blockers placed at 6, 8, and 10 mm from the target surface at lower pressure values of 5 and 10 Torr (first regime), maximum enhancement of electron temperature and electron number density is obtained for blocker distance of 8 mm, then for 10 mm, and minimum for 6 mm. This can be attributed to change in plume shape due to presence of blockers at these distances. For the blocker distance of 6 mm, shock waves reflect back from the closer surface immediately, while bouncing back they exert a higher pressure than blocker at higher distance of 8 and 10 mm. These reflected shock waves move towards the plasma plume with higher force and after compression and confinement they deform the plasma. Final shape of plasma becomes narrower and more elongated. Therefore, 6 mm blocker distance produces less significant effects on enhancement of plasma parameters because of its higher pressure and de-shaping the plume resulting in lesser

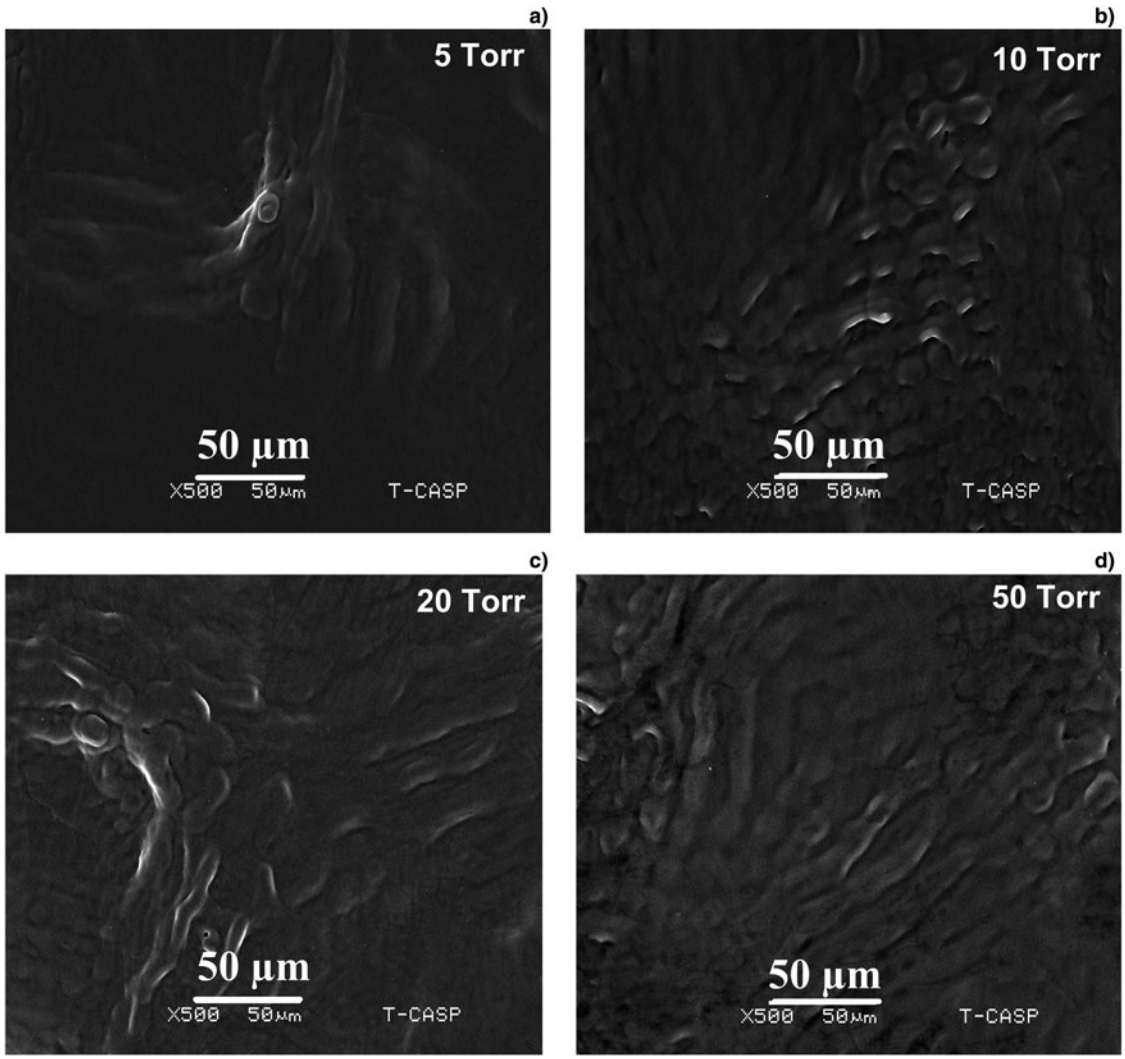

Fig. 7. SEM micrographs revealing the surface morphology of central ablated regions of Mg exposed to 50 laser shots at fluence of 18 J/cm^2 without blocker at various pressures of (a) 5 Torr, (b) 10 Torr, (c) 20 Torr, and (d) 50 Torr.

https://doi.org/10.1017/S0263034617000210 Published online by Cambridge University Press

involvement of plasma particles in collisional excitation in the central region of plasma (Gao *et al.*, 2015). While comparing the blocker distance of 8 and 10 mm, the reason for maximum values of plasma parameters obtained for the blocker distance of 8 mm is explained as the propagating shock waves require less time to encounter and reflect back earlier from the blocker placed at closer distance, while confines the plasma plume efficiently and results in enhanced electron temperature and electron number density.

For second regime dealing with higher pressures of 20 and 50 Torr, the best confinement results with highest temperature and number density plasma are obtained with blocker distance of 6 mm as compared with 8 and 10 mm. The reason is explainable on the basis of fact that at higher pressures, the plume length becomes shorter due to confinement effect offered by Ar gas. Therefor, 6 mm becomes appropriate distance for offering the best confinement effect through combination of shock waves and gas confinement as compared with 8 and 10 mm. At higher pressures of 20 and 50 Torr, the pressure of shock waves on plasma plume is comparatively less effective as compared with the pressure offered at lower pressures of 5 and 10 Torr. As plasma already significantly compressed and confined due to high Ar pressure, therefore shock waves cannot deform the plume shape. Hence, the small blocker distances are found to be more suitable for providing the better confinement effects at higher ambient pressures.

Moreover, the experiments are also performed for the Ar pressure of more than 50 Torr and for blocker distance <6 mm. No significant enhancement of plasma parameters has been observed. The effects of spatial confinement offered by blocker are not observed for the blocker distance <6 mm and for the pressure of Ar >50 Torr and therefore these results are not presented.

3.2. SEM analysis

3.2.1. Effect of Ar gas pressure on surface morphology of laser-irradiated Mg

In order to correlate the surface modifications of laser-ablated Mg with plasma parameters, one fluence value is

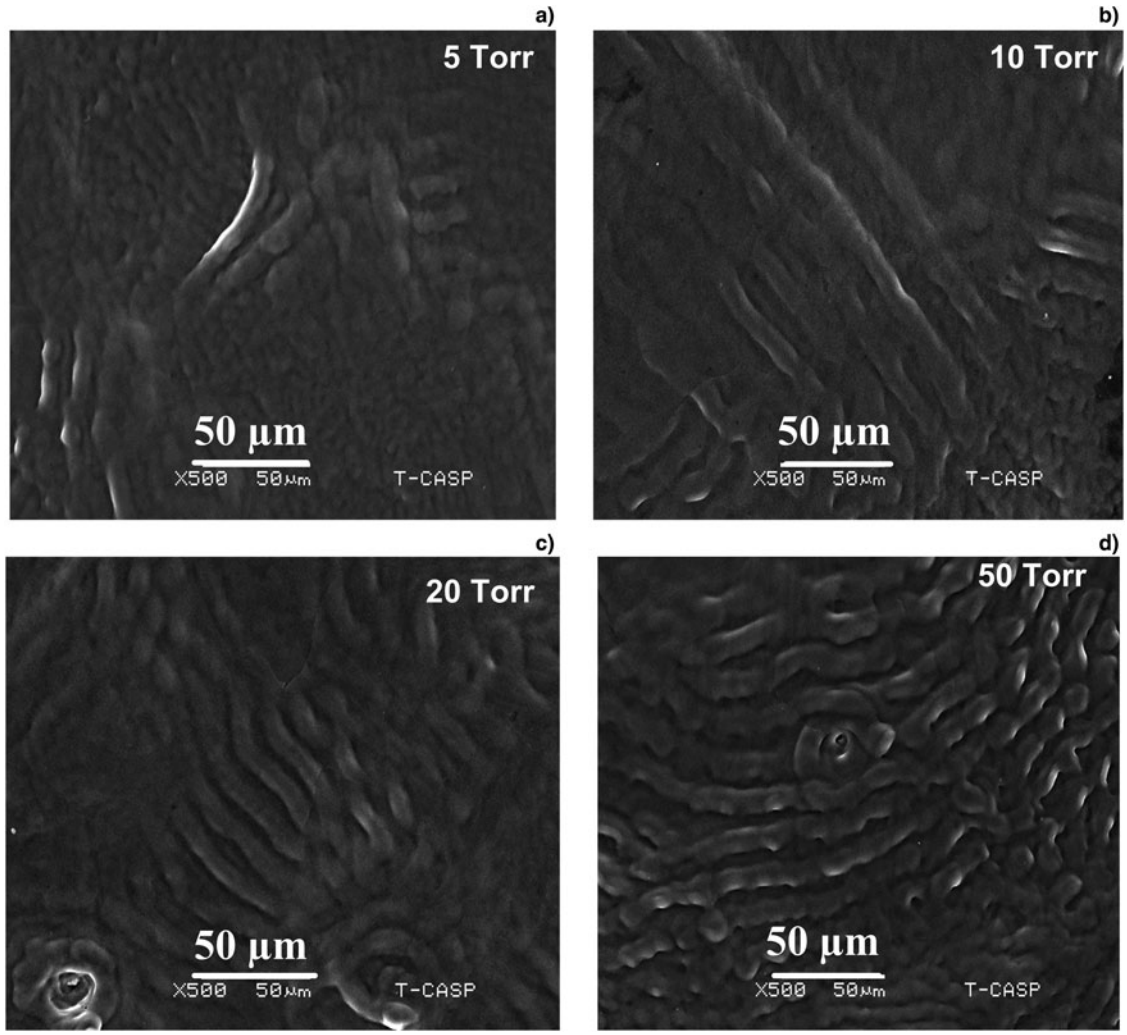

Fig. 8. SEM micrographs revealing the surface morphology of central ablated regions of Mg exposed to 50 laser shots at fluence of 18 J/cm^2 with blocker at distance of 6 mm at various pressures of (a) 5 Torr, (b) 10 Torr, (c) 20 Torr, and (d) 50 Torr.

https://doi.org/10.1017/S0263034617000210 Published online by Cambridge University Press

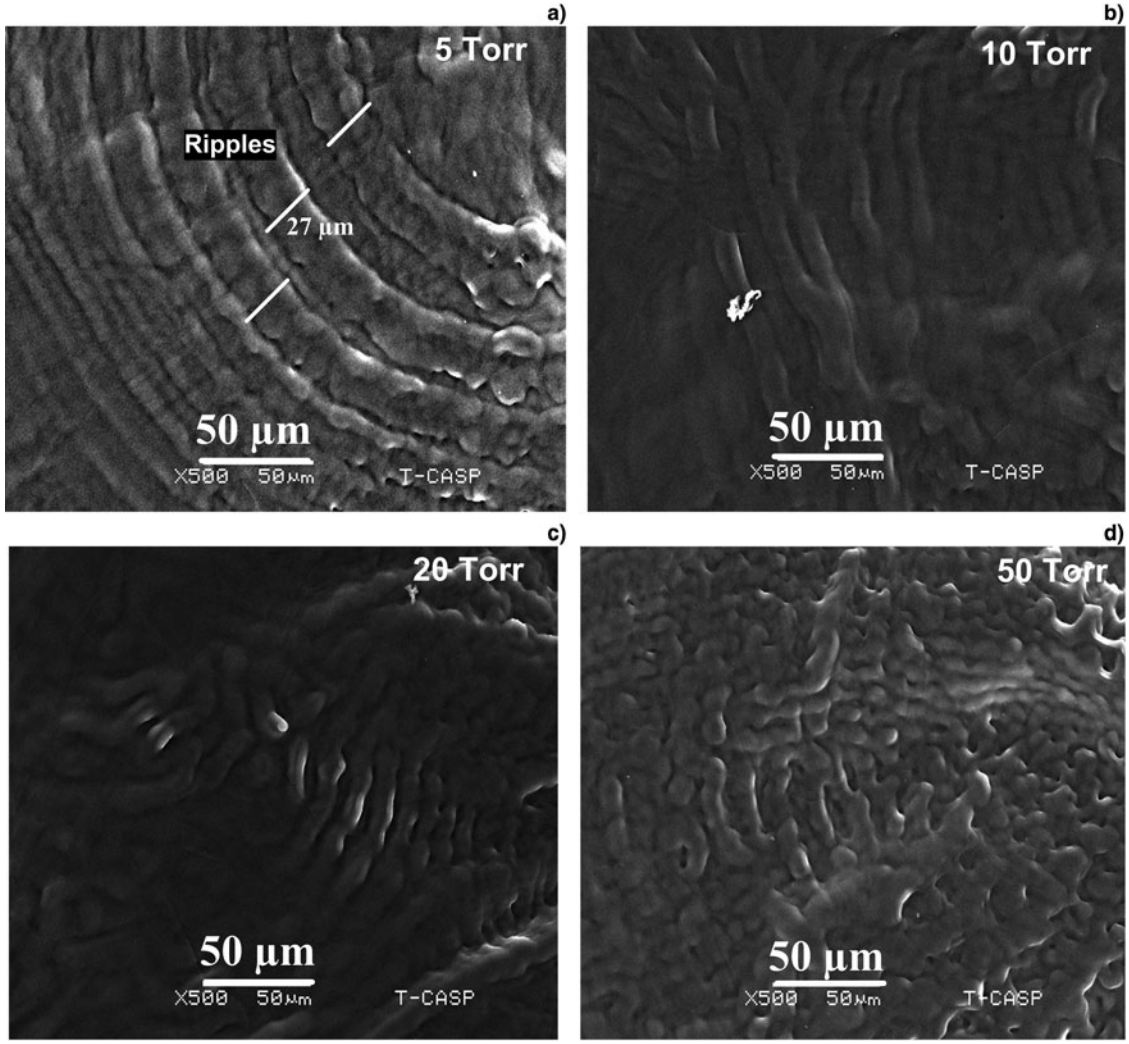

Fig. 9. SEM micrographs revealing the surface morphology of central ablated regions of Mg exposed to 50 laser shots at fluence of 18 J/cm^2 with blocker at distance of 8 mm at various pressures of (a) 5 Torr, (b) 10 Torr, (c) 20 Torr, and (d) 50 Torr.

selected that corresponds to the maximum excitation temperature of Mg plasma and the SEM micrographs corresponding to this fluence are presented in Figures 7–10 at various pressures ranging from 5 to 50 Torr. All SEM results of Figures 7–10 reveal the surface modification after laser ablation of Mg in the absence and in the presence of blockers at various distances of 6, 8, and 10 mm, respectively at Ar pressure of (a) 5 Torr, (b) 10 Torr, (c) 20 Torr, and (d) 50 Torr. These figures depict that pressure variation significantly influences the surface structuring of irradiated Mg. It is clearly seen from these figures at higher fluence of 18 J/cm^2, there is large-scale melt expulsion towards boundaries resulting in formation of ripples, channels, and wavy patterns.

When laser interacts with material surface, non-uniform energy deposition and absorption take place due to voids, inhomogeneities, material impurities, and surface roughness (Bashir *et al.*, 2009). The surface modification of laser-ablated Mg can be well correlated with plasma temperature and electron number density. At high laser fluence of 18 J/cm^2, the ablation rate increases with more energy deposition resulting in higher electron temperature and number density ranging from 6146 to 1193 K and 1.2×10^{16} to 3.5×10^{16} cm^{-3} which causes the large-scale melting and vaporization. The melt flow becomes more turbulent, whereas ripples and channels become more diffusive at higher pressure of 50 Torr as shown in Figures 7a–7d and 10a–10d. This variation in structural features with increasing pressure is explainable on the basis of plasma parameters. When Ar pressure increases from 5 to 20 Torr, electron temperature and electron number density are also increased due to plasma confinement through ambient pressure. The increasing values of electron temperature and electron number density with increasing pressure produce more heating and melting on target surface due to more energy deposition to the lattice resulting in turbulent flow from center toward the boundaries. Therefore, channels and ripples

https://doi.org/10.1017/S0263034617000210 Published online by Cambridge University Press

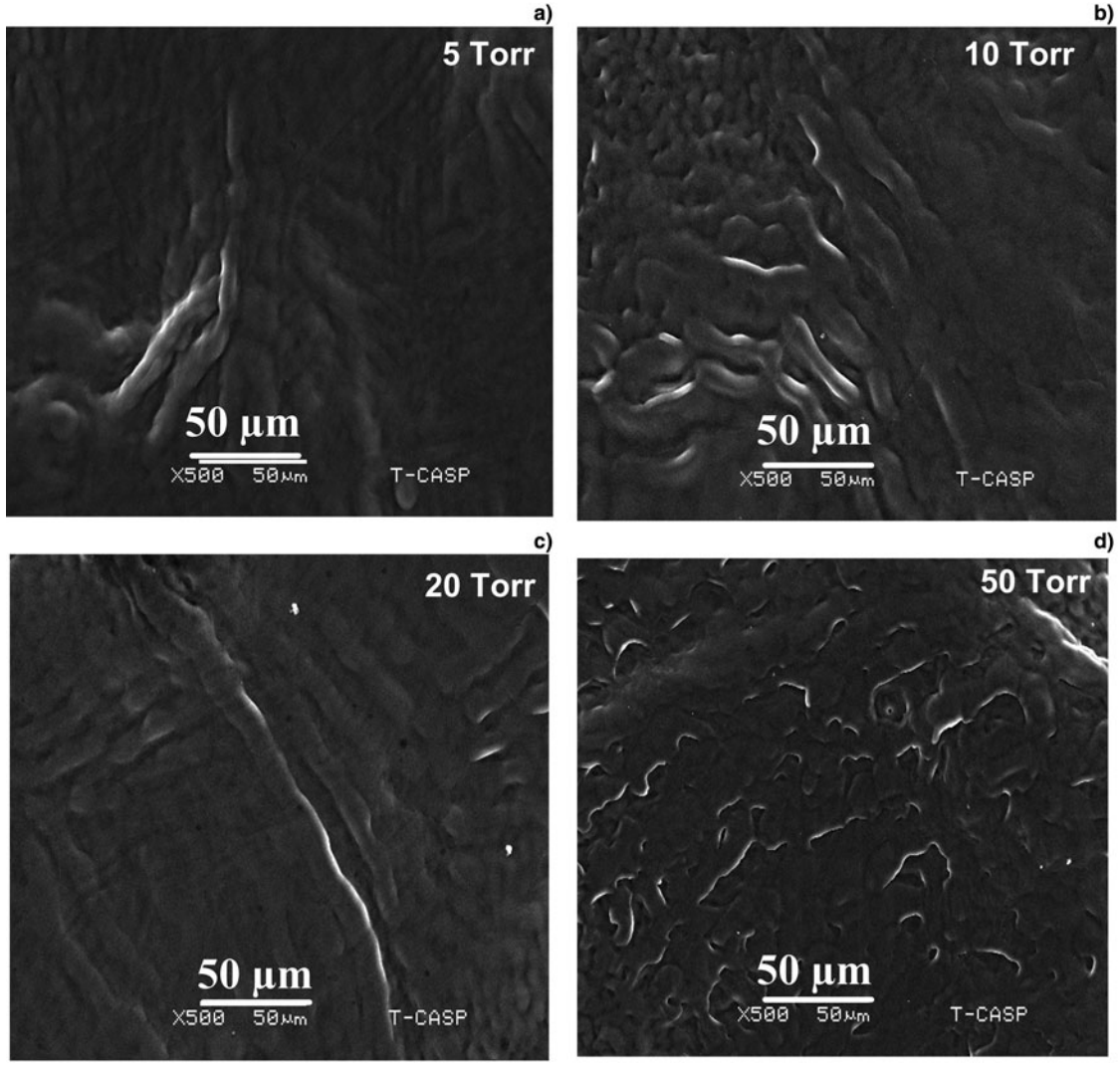

Fig. 10. SEM micrographs revealing the surface morphology of central ablated regions of Mg exposed to 50 laser shots at fluence of 18 J/cm^2 with blocker at distance of 10 mm at various pressures of (a) 5 Torr, (b) 10 Torr, (c) 20 Torr, and (d) 50 Torr.

become more diffusive at target surface at higher pressures. It is reported (Iqbal *et al.*, 2012) that the high-temperature plasma exerts a pressure up to GPa on the target surface and plays a crucial role on surface morphology. This consideration emphasizes that both plasma pressure and shock waves derive the turbulent flow of the molten material by enhancing the melting effect finally suppressing the surface features.

3.2.2. Effect of metal blocker and its distance on surface morphology of laser-irradiated Mg

In order to explore the effect of spatial confinement offered by blocker placed at various distances on the surface modification of laser-ablated Mg, the results are summarized in SEM micrographs of Figures 7–10, (Fig. 7) in the absence of blocker and at the blocker distance of (Fig. 8) 6, (Fig. 9) 8, and (Fig. 10) 10 mm. It is clear from these figures that not only the presence of blocker, but also its distance from the target produces a significant effect on surface morphology of Mg. The observations of the SEM images reveal that that there is pronounced formation of ripples and channels in the presence of blocker. These ripples become more organized and well defined at a distance of 8 mm (Fig. 9a) as compared with 6 and 10 mm blocker distance. This is valid for lower pressures of 5 and 10 Torr. When the pressures is increased to 20, the blocker distance of 6 mm offers more pronounced spatial confinement as compared with 8 and 10 mm and results in comparatively distinct organized ripples formation (Fig. 8c). It implies that there is a unique combination of pressure and blocker distance for each fluence, which is responsible for the maximum electron temperature and number density of Mg plasma due to maximum compression and confinement. The periodicity of ripples formed at both pressures of 5 and 10 Torr at 8 mm blocker distance is calculated as 27 and 17.4 µm, respectively, and

https://doi.org/10.1017/S0263034617000210 Published online by Cambridge University Press

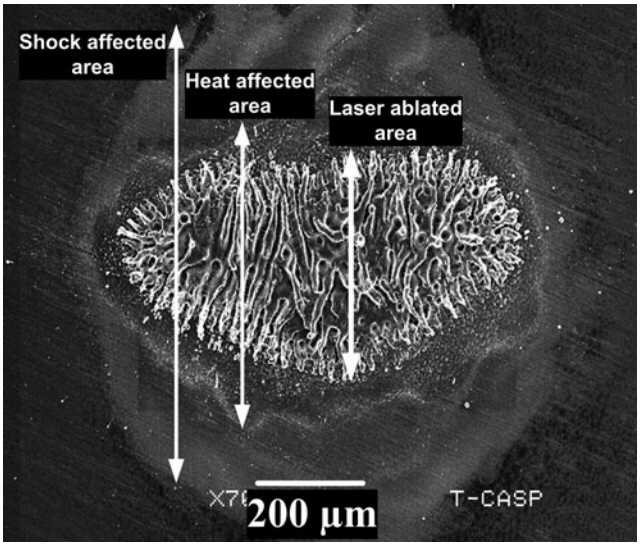

Fig. 11. SEM micrograph representing the laser-irradiated spot area and shock affected area of Mg exposed to 50 shots at laser fluence of 18 J/cm^2 with blocker at a distance of 8 mm under fixed Ar pressure of 20 Torr.

is attributed to maximum electron temperature and electron number density.

Both the laser fluence and presence of blocker also plays a significant role on laser-ablated spot area also called laser-irradiated area and shock-affected area. When laser interacts with materials, three kinds of regions are formed as (i) laser-ablated area at which the ablation and plasma formation occur, (ii) heat-affected area which is region over which material changes its properties as a result of heat conduction during and after the laser pulse, and (iii) the third one is shock-affected region which is formed due to energy deposition through shock waves (Bauerle, 2011). The laser-ablated and shock-affected regions of laser-ablated Mg are shown in Figure 11. These areas are measured by SEM analysis and are listed in Table 2 for both without and with blocker cases. From Table 2, it is clear that the laser-ablated area decreases, whereas the heat-affected area increases in the presence of blocker for all measurements. This is attributed to enhanced confinement effect offered by blocker that finally reduces the laser spot area and increases the shock-affected areas. These reduced laser-irradiated areas in turn produce high-temperature and high-density plasma in localized region and is responsible for distinct surface morphological features.

4. CONCLUSIONS

The effect of spatial confinement offered by Ar pressure and metallic blocker on plasma parameters and surface modifications of Mg is investigated. LIBS analysis reveals that both electron temperature and electron number density are strongly dependent upon ambient pressure. Electron temperature increases with increasing pressure, attain its maxima at the pressure of 20 Torr, then decreases at maximum pressure of 50 Torr; whereas electron number density continuously increases up to maximum value of Ar pressure. SEM investigations reveal the ripples and channel formation. The presence of blocker and its distance significantly affect the electron temperature and electron number density, surface morphology and shock-affected regions around laser spot area. At lower pressures of 5 and 10 Torr, 8 mm blocker distance is found to be optimum for maximum enhancement of electron temperature and electron number density and cleaner ablation with distinct ripple formation. At higher pressures of 20 and 50 Torr, 6 mm blocker distance produces a significant role for enhancing electron temperature and electron number density. The enhancement in plasma parameters and surface morphological development is attributed to confinement effect through shock waves that hinders the free expansion plasma. The more collisions, excitations and de-excitations among plasma in confined region finally results in higher electron temperature and electron number density with more distinct as well as well-defined surface features in the presence of blocker. The optimum combination of laser fluence along with Ar pressure and spatial confinement offered by blocker distance can make Mg plasma more suitable and beneficial for ion implantation, thin-film deposition and micro/nano-structuring of materials.

Table 2. *Average values of laser irradiated spot areas and shock affected areas calculated from SEM analysis under various Ar pressures ranging from 5–50 Torr at laser fluence 18 J/cm^2 (corresponding to maximum electron temperature).*

Pressure (Torr)		Higher laser fluence, 18 J/cm^2			
		Without blocker	With blocker at 6 mm	With blocker at 8 mm	With blocker at 10 mm
5	Laser-ablated area ($\times10^{-4}$ cm^2)	193	189	184	187
	Shock-affected area ($\times10^{-4}$ cm^2)	1831	2157	1519	2038
10	Laser-ablated area ($\times10^{-4}$ cm^2)	185	177	182	180
	Shock-affected area ($\times10^{-4}$ cm^2)	1699	1900	1854	1704
20	Laser-ablated area ($\times10^{-4}$ cm^2)	128	125	112	155
	Shock-affected area ($\times10^{-4}$ cm^2)	1589	1449	1766	1618
50	Laser-ablated area ($\times10^{-4}$ cm^2)	124	120	109	148
	Shock-affected area ($\times10^{-4}$ cm^2)	1385	2640	2613	2344

https://doi.org/10.1017/S0263034617000210 Published online by Cambridge University Press

ACKNOWLEDGMENT

Authors are thankful to Higher Education Commission (HEC) of Pakistan for funding the project "Upgradation of Laser lab facilities" at CASP, GC University, Lahore.

REFERENCES

Bashir, S., Rafique, M.S. & Husinsky, W. (2009). Surface topography (nano-sized hillocks) and particle emission of metals, dielectrics and semiconductors during ultra-short-laser ablation: Towards a coherent understanding of relevant processes. *Appl. Surf. Sci*. **255**, 8372–8376.

Bauerle, D. (2011). *Laser Processing and Chemistry*. Heidelberg: Springer-Verlag.

Chen, F.F., Su, X.J. & Zhou, W.D. (2015). Effect of parameters on Si plasma emission in collinear double-pulse laser-induced breakdown spectroscopy. *Front. Phys*. **10**, 104207–10412.

Chorlis, C.H., Reader, J., Wiese, W.L. & Martin, G.A. (1980). *Wavelengths and Transition Probabilities for Atoms and Atomic Ions*. Washington, DC: National Bureau of Standards.

Cremer, D.A. & Radziemski, L.J. (2006). *Handbook of Laser-Induced Breakdown Spectroscopy.* Chichester: Wiley.

Dawood, A., Bashir, S., Akram, M., Hayat, A., Ahmad, S., Iqbal, M.H. & Kazmi, A.H. (2015). Effect of nature and pressure of ambient environments on the surface morphology, plasma parameters, hardness, and corrosion resistance of laser-irradiated Mg-alloy. *Laser Part. Beams* **33**, 315–330.

Dawood, M.S. & Margot, J. (2014). Effect of ambient gas pressure and nature on the temporal evolution of aluminium laser-induced plasmas. *AIP Adv*. **4**, 0371111–0371113.

Farid, N., Harilal, S., Ding, H. & Hassanein, A. (2014). Emission features and expansion dynamics of nanosecond laser ablation plumes at different ambient pressures. *J. Appl. Phys*. **115**, 033107–033116.

Fried, D., Khshida, T., Reck, G.P. & Rothe, E.W. (1992). Effect of electric field associated with a laser induced pulsed discharge on the ablation-generated plumes of YBa2Cu3O7-X. *J. Appl. Phys*. **72**, 1113–1125.

Fu, Y., Hou, Z. & Wang, Z. (2016). Physical insights of cavity confinement enhancing effects in laser-induced breakdown spectroscopy. *Opt. Exp*. **24**, 3055–3066.

Gao, X., Liu, L., Song, C. & LIN, J. (2015). The role of spatial confinement on nanosecond YAG laser-induced Cu plasma. *J. Phys. D: Appl. Phys*. **48**, 1752051–1552056.

Harilal, S.S., Bindhu, C.V., Nampoori, V.P.N. & Vallabhan, C.P.G. (1998). Influence of ambient gas on the temperature and density of laser produced carbon plasma. *Appl. Phys. Lett*. **72**, 167–169.

Harilal, S.S., Farid, N., Freeman, J.R., Diwakar, P.K., Lahaye, N.L. & Hassanein, A. (2014). Background gas collisional effects on expanding fs and ns laser ablation plumes. *Appl. Phys. A* **117**, 319–326.

Hayat, A., Bashir, S., Rafique, M.S., Akram, M., Mahmood, K., Iqbal, S., Dawood, A. & Arooj (2016). Spectroscopic and morphological study of laser ablated Titanium. *Opt. Spectrosc*. **121**, 1–9.

Huang, F., Liang, P., Yang, X., Cai, H., Wu, J., Ying, Z. & Sun, J. (2015). Confinements effects of shock waves on laser-induced plasma from graphite target. *Phys. Plasmas* **22**, 063509–063516.

Iqbal, S., Rafique, M.S., Anjum, S., Hayat, A. & Iqbal, N. (2012). Impact of X-ray irradiation on PMMA thin films. *Appl. Surf. Sci*. **259**, 853–860.

Khalil, A.A.I. & Gondal, M.A. (2012). Effect of ambient conditions on laser induced breakdown spectroscopy. *Laser Phys*. **22**, 1771–1779.

Khumaeni, A., Akaoka, K., Miyabe, M. & Wakaida, I. (2016). The role of microwaves in the enhancement of laser-induced plasma emission. *Front. Phys*. **11**, 1142092–1142099.

Liu, L., Huang, X., Li, S., Lu, Y., Chen, K., Jiang, L., Silvain, J.F. & Lu, Y.F. (2015). Laser-induced breakdown spectroscopy enhanced by a micro torch. *Appl. Opt*. **23**, 15047–15057.

Rumsby, P. & Paul, J.W.M. (1974). Temperature and density of an expanding laser produced plasma. *J. Plasma Phys*. **16**, 247–251.

Scaffidi, J., Pender, J., Pearman, W., Goode, S.R., Colston, B.W., Carter, J.C. & Angel, S.M. (2003). Dual-pulse laser-induced breakdown spectroscopy with combinations of femtosecond and nanosecond laser pulses. *Appl. Opt*. **42**, 6099–6106.

Shakeel, H., Arshad, S., Haq, S.U. & Nadeem, A. (2016). Electron temperature and density measurements of laser induced germanium plasma. *Phys. Plasmas* **23**, 0535041–0535049.

Verhoff, B., Harilal, S.S., Freeman, J.R., Diwakar, P.K. & Hussanein, A. (2012). Dynamics of femto-and nanosecond laser ablation plumes investigated using optical emission spectroscopy. *J. Appl. Phys*. **112**, 0933031–0933039.

Zhong, S.L., Lu, Y., Kong, W.J., Cheng, K. & Zheng, R. (2016). Quantitative analysis of lead in aqueous solutions by ultrasonic nebulizer assisted laser induced breakdown spectroscopy. *Front. Phys*. **11**, 1142021–1142029.